Optimal flow metering and lane-changing control with ramp-metering saturation

Farzam Tajdari, Hasan Ramezanian, Shadi Paydarfar, Ali Lashgari, Shakib Maghrebi

Flow metering and lane-changing optimal control with ramp-metering saturation

Farzam Tajdari
School of Engineering
Aalto University
Espoo, Finland
farzam.tajdari@aalto.fi

Hasan Ramezanian
Department of Mechanical Engineering
Amirkabir University of Technology
Tehran, Iran
h_ramezanian@yahoo.com

Shadi Paydarfar
Medical Immunology, School of Medicine
Shahid Beheshti University
Tehran, Iran
shadipaydarfar.91@gmail.com

Ali Lashgari
Department of Economics
Kansas State University
Kansas, USA
alilashgari@ksu.edu

Shakib Maghrebi
Department of Electrical Engineering
Abbaspour - Shahid Beheshti University
Tehran, Iran
shakibology80@gmail.com

***Abstract*—To accomplish a successful transportation framework, we present a novel methodology for incorporating lane-changing and ramp-metering control, which exploits the presence of connected and partially autonomous vehicles. The primary test tended to is coordinating the ramp-metering flow saturation boundaries in the optimal controller. Specifically, i t i s expected that a level of vehicles can get and carry out explicit control assignments (e.g., lane-changing control signals). Utilizing a Linear Quadratic Integral (LQI) controller and an anti-windup plan in view of a LTI model, another methodology is introduced for powerfully expanding the throughput at motorway bottlenecks. In terms of assessment, the methodology is implemented on the simulated model, performed on a first-order, multi-lane, macroscopic traffic fl ow mo del. Th e ca pacity dr op peculiarity is additionally executed, that addresses the effect of the created method to deal with be demonstrated, same as the improvements in rush hour traffic effectiveness.**

***Index Terms*—Lane-changing, Ramp-metering, Saturation, Optimal control, Connected and automated vehicles.**

I. Introduction

In recent decades, the automotive industry and enormous academic institutions around the world have devoted a significant and growing interdisciplinary effort to arranging, creating, testing, and sending new advancements that are relied upon to reform the highlights and capacities of individual vehicles later on [1]. Among the several available solutions, only a handful may have a direct influence o n t raffic flo w, while the vast majority are solely concerned with increasing driver safety or convenience [2]–[7]. Only a few publications in the context of autonomous vehicle and connected vehicles have investigated optimizing lane distribution [8]. Several previous works particularly addressed the challenge of determining effective vehicle lane-paths for a motorway under fully automated or semi-automatic driving [8]. A feedback-based optimal controller [9]–[12] regarding lane-changing control is structured in [13] as a Linear Quadratic Regulator (LQR), reaches various traffic d ensity d istribution a t t he motorway bottleneck regarding the different lanes. However, another controller is anticipated in the work to guarantee that the total traffic flow entering the region where lane-changing control is utilized does not altogether surpass the bottleneck limit. This paper elaborates the results in [14] considering the presence of partially autonomous and networked vehicles, proposing a unique way for combined lane-changing and saturated ramp-metering control. The remainder of this paper includes, first definition of the used traffic flow model in Section II. Then, the proposed controller is introduced in Section III. Section IV explains the test-bed configurations, and in Section V the experiment outcomes are discussed. Section VI concludes the paper and the future research directions are highlighted as well.

II. Linear Multi-Lane Traffic Flow Model

A N segmented multi-lane highway is used, indexed by $i = 0, \ldots, N$, of length L_i,and each segment is composed of lanes, indexed by $j = m_i, \ldots, M_i$, that m_i and M_i are the minimum and maximum indexes of lanes for segment i defines each element of the resulting network (shown in Fig. 1) entitled "cell", that is named by (i, j). To consider different network topology, containing lane decreases and lane increase on the right and left sides of the highway, it is assumed that $j = 0$ corresponds to the segment(s) containing the right-most lane. For instance, considering the motorway network showed in Fig. 1, $m_0 = 0$ and $M_0 = 4$, while $m_3 = 1$ and $M_3 = 3$. The model is structured in discrete time, including the time step T, indexed by $k = 0, 1, \ldots$, that the time is $t = kT$. The total number of cells, according to this description, is $H = \sum_{r=0}^{N} (M_r - m_r + 1)$ and the number of cells placed at the bottleneck area is $S = M_N - m_N + 1$. Each motorway cell (i, j) is featured via the traffic density $\rho_{i,j}(k)$ (equals to the number of vehicles in the cell divided by L_i). Dynamically, density changes based on the conservation law equation as below, see, for example [14],

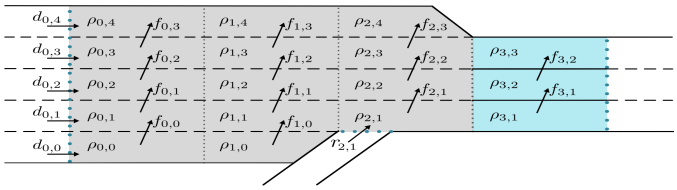

Fig. 1: A hypothetical motorway stretch.

$$\rho_{i,j}(k+1) = \rho_{i,j}(k) + \frac{T}{L_i}\left[q_{i-1,j}(k) - q_{i,j}(k)\right] + \frac{T}{L_i}\left[f_{i,j-1}(k) - f_{i,j}(k)\right] + \frac{T}{L_i} d_{i,j}(k) + \frac{T}{L_i} r_{i,j}(k), \quad (1)$$

where $q_{i,j}(k)$ represents the longitudinal flow exiting from cell (i,j) and penetrating to cell $(i+1,j)$ during the time interval $(k,k+1]$; $f_{i,j}(k)$ is the net lateral flow going from cell (i,j) to cell $(i,j+1)$ during time interval $(k,k+1]$; and $d_{i,j}(k)$ is any external flow entering the network in cell (i,j) during time period $(k,k+1]$, either from upstream of the considered stretch or from an on-ramp. Because a ramp is supposed to be controlled, we name $r_{i,j}(k)$ as the inflow able to enter the network from the ramp positioned in (i,j) during time interval $(k,k+1]$ (e.g., $r_{2,1}$ in Fig. 1). Some terms of (1) may not be considered depending on the network topology. The inflow $q_{i-1,j}(k)$ does not present for the first segment of the network, the outflow $q_{i,j}(k)$ does not present for the final segment prior a lane-drop, and the lateral flow terms $f_{i,j}(k)$ present just for $m_i \leq j < M_i$. Based on the preceding assumptions, the whole number of lateral flow terms is $F = H - N$. Consider the familiar relationship

$$q_{i,j}(k) = \rho_{i,j}(k)\; v_{i,j}(k). \quad (2)$$

Because the controller is intended to work in congested traffic conditions, we assume that the speed in all cells remains constant (e.g., the critical speed) $v_{i,j}(k) \equiv \bar{v}_{i,j}, \forall i,j,k$. Despite the fact that this appears to be a strong assumption, it will be mentioned in simulation (Section V) where the controller reaches acceptable performance also when speed changes over time. As a result, we can define the resultant system as a Linear Time Invariant (LTI) system by replacing (2) with (1)

$$\bar{x}(k+1) = \bar{A}\bar{x}(k) + \bar{B}u(k) + \bar{d}(k) \quad (3)$$

where (time index k is omitted to simplify notation)

$$\bar{x} = [\rho_{0,m_0} \dots \rho_{0,M_0}\;\; \rho_{1,m_1} \dots \rho_{N,M_N}]^T \in \mathbb{R}^H, \quad (4)$$

$$\bar{d} = \left[\frac{T}{L_0} d_{0,m_0} \dots \frac{T}{L_0} d_{0,M_0}\;\; \frac{T}{L_0} d_{1,m_1} \dots \frac{T}{L_0} d_{N,M_N}\right]^T \in \mathbb{R}^H, \quad (5)$$

$$u = [f_{0,m_0} \dots f_{0,M_0}\; f_{1,m_1} \dots f_{N,M_N}, r_{i,j}]^T \in \mathbb{R}^{F+1}. \quad (6)$$

Variables u and $\bar{d}$ are the controlled and disturbance inputs, respectively; u contains all the lateral flows $f_{i,j}$ and the ramp flow $r_{i,j}$ that is supposed to be controllable, on the other hand $\bar{d}$ contains the external flows that are not in u. Matrix $\bar{A} \in \mathbb{R}^{H \times H}$, composed of elements $a_{\bar{p},\bar{s}}$, it shows the connections formed by a longitudinal flow between pairs of succeeding cells. Finally, matrix $\bar{B}$, composed of elements $b_{\bar{p},\bar{s}}$ it reflects the interconnections between cells via their lateral fluxes entering and exiting. Therefore, the matrices for the aforementioned system can be described as follows:

$$a_{\bar{p},\bar{s}} = \begin{cases} 1 & \text{if } \bar{p} = \bar{s} \text{ and } (j < m_{i+1} \text{ or } j > M_{i+1}) \\ 1 - \frac{T}{L_i}\bar{v}_{i,j} & \text{if } \bar{p} = \bar{s} \text{ and } (i = N \text{ or } m_{i+1} \leq j \leq M_{i+1}) \\ \frac{T}{L_i}\bar{v}_{i,j} & \text{if } \bar{p} > H_0 \text{ and } \bar{s} = \bar{p} - M_{i-1} + m_i - 1 \\ 0 & \text{otherwise} \end{cases} \quad (7)$$

$$b_{\bar{p},\bar{s}} = \begin{cases} \frac{T}{L_i} & \text{if } j > m_i \text{ and } \bar{s} = \bar{p} - i \\ -\frac{T}{L_i} & \text{if } j < M_i \text{ and } \bar{s} = \bar{p} - i + 1 \\ \frac{T}{L_i} & \text{if } j = \bar{j} \text{ and } i = \bar{i} \\ 0 & \text{otherwise} \end{cases} \quad (8)$$

where $(\bar{i},\bar{j})$ explains the location of on-ramp flow.

At the end, it is noted that the CFL condition [14] is considered as

$$\frac{T}{L_i}\bar{v} < 1 \quad (9)$$

should be followed in order to create a realistic discrete time [15], [16] and discrete space traffic flow model.

III. Integrated Ramp-Metering and Lateral Flow Controller

A. Formulation

The linear system described in Section II is used here to design an optimal control problem, the solution of which leads to a MIMO (multi-input multi-output) feedback controller [17]. Specifically, the controller should handle lateral flows as well as flow entering from an on-ramp located upstream of the bottleneck in order to avoid congestion and maximize bottleneck throughput.

To maximize bottleneck throughput, densities at bottleneck areas should be kept close to their critical values ($\rho^{cr}_{S\times 1}$), which are assumed to be known here. To avoid offset at the stationary state in the presence of disturbances (e.g., upstream mainstream demand or uncontrolled lateral flows), we apply an integral controller to reject constant disturbances [14], [18], thus eliminating the requirement to measure the external inflows. We structure the problem by augmenting the original system (3) with S (i.e, equal to the bottleneck lanes) integral states, defined as z, where

$$z(k+1) = z(k) + \bar{C}\bar{x}(k) - \rho^{cr}. \quad (10)$$

The resulting augmented system will be as

$$x(k+1) = Ax(k) + Bu(k) + d(k), \quad (11)$$

where

$$x = \begin{bmatrix} \bar{x} \\ z \end{bmatrix}, \quad d = \begin{bmatrix} \bar{d} \\ -\rho^{cr}_{S\times 1} \end{bmatrix}, \quad A = \begin{bmatrix} \bar{A} & 0_{H\times S} \\ \bar{C} & I_{S\times S} \end{bmatrix}, \quad (12)$$

$$B = \begin{bmatrix} \bar{B} \\ 0_{S\times(F+1)} \end{bmatrix}, \quad \bar{C} = \begin{bmatrix} 0_{S\times(H-S)} & I_{S\times S} \end{bmatrix}. \quad (13)$$

Over an infinite time horizon, we define the quadratic cost function shown below, which provides for the penalization of integral states and control inputs:

$$J = \sum_{k=0}^{\infty} \left[x^T(k) C\; Q\; C^T x(k) + u^T(k)\; R\; u(k)\right], \quad (14)$$

where

$$Q = w_Q\ I_{S\times S}, \quad R = \begin{bmatrix} w_{R_1}\ I_{F\times F} & 0_{F\times 1} \\ 0_{1\times F} & w_{R_2} \end{bmatrix} \tag{15}$$

$$C = \left[\ 0_{S\times H}\ \vdots\ I_{S\times S}\ \right]. \tag{16}$$

Matrices Q and R are weighting matrices employed to magnify the integral states and control commands, respectively, explained via parameters $w_Q > 0$, $w_{R_1} > 0$, and $w_{R_2} > 0$. The optimal control problem addresses (14), (11) can be solved by a LQR, that gives a stabilizing feedback gain assuming that the original system is at least stable and noticeable [14], [19], [20], that can be assessed employing, e.g, the Hautus-test [21]. Also, the stability of the system is comprehensively studied in [14].

B. Controller design

The linear feedback control law is the answer to the proposed LQR problem [22]

$$u(k) = -Kx(k), \tag{17}$$

where

$$K = \left(R + B^T P B\right)^{-1} B^T P A \tag{18}$$

$$P = C^T Q C + A^T P A - A^T P B \left(R + B^T P B\right)^{-1} \tag{19}$$

The optimal result (18) and the Algebraic Riccati Equation (19) are extensively discussed in [14]. The feedback control law (17) is quite useful in practice, since the computation of offline manipulation of the feedback gain matrix K is possible. Practical-wise, the gain K may be properly split as

$$K = \left[\ K_P\ \vdots\ K_I\ \right], \tag{20}$$

that let us to reformulate the control law as

$$u(k) = -K_P\ \bar{x}(k) - K_I\ z(k). \tag{21}$$

In practice, it may not always be possible to obtain the intended density set-point at the bottleneck (for example, due to input saturation); hence an anti-windup technique must be included in our controller. We use the proposed method in [14], that, in this case, modifies the dynamic controller's integral part (10) as

$$z(k+1) = (I + MK_I)z(k) + \left(\bar{C} + MK_P\right) x(k) + Mu_{\text{sat}}(k). \tag{22}$$

The saturated input u_{sat} is explained as

$$u_{\text{sat}}(k) = \text{sat}(u(k)) \tag{23}$$

$$\text{sat}(u_m) = \begin{cases} u_m^{\min} & \text{if } u_m < u_m^{\min} \\ u_m^{\max} & \text{if } u_m > u_m^{\max} \\ u_m, & \text{otherwise,} \end{cases} \tag{24}$$

where m is the index of the element inside vector u, and $u_m^{\min}$ and $u_m^{\max}$ are the lower and upper bound for the input u_m. Matrix M should be selected in such a way that $I + MK_I$ has stable eigenvalues, for example, using classical pole placement. Stability of the closed-loop system (3), (21)-(24) can be investigated through the results from [23].

C. Problem design with input saturation of bottleneck area

To design a controller for saturated input, we use a constant upper-bound (a) as a restriction for the on-ramp input and recast the Hamiltonian equation [24] as following:

$$r_{2,1} \leq a \tag{25}$$

$$f_{N+1} = r_{2,1} - a \tag{26}$$

$$\mathcal{H} = \frac{1}{2}x^T Q x + \frac{1}{2}u^T R u + \sum_{i=1}^{N} \lambda_i f_i + \lambda_{N+1} f_{N+1} \tag{27}$$

where f_{N+1} is a function that defines the constraint violation. Then, we present an extra state x_{N+1} representing the integral of the difference between the on-ramp flow and its upper-bound.

$$x_{N+1}(k+1) = x_{N+1}(k) + T\frac{\partial \mathcal{H}}{\partial \lambda} = x_{N+1}(k) + T f_{N+1}(k) \tag{28}$$

We now determine a new augmented system considering

$$\underline{\tilde{x}}^n = \begin{bmatrix} \underline{x} \\ \underline{x}_{N+1} \\ z \end{bmatrix}, \underline{\tilde{u}}^n = \underline{\tilde{u}}, \underline{d}^n = \begin{bmatrix} \bar{d} \\ \bar{0} \\ -\bar{\rho}_{S\times 1}^{cr} \end{bmatrix} \tag{29}$$

To find the new A, B and C matrix of dynamic equation, $r_{2,1}$ must be defined based on either the states or the inputs, thus from the previous section we have:

$$r_{2,1} = u(3,k) \tag{30}$$

$$\underline{\tilde{A}}_1^n = \begin{bmatrix} A & 0_{H\times 1} & 0_{H\times S} \\ 0_{1\times H} & 1 & 0_{1\times S} \\ C & 0_{S\times 1} & I_{S\times S} \end{bmatrix}, \underline{\tilde{B}}_1^n = \begin{bmatrix} B \\ 0_{1\times F} \\ 0_{S\times(F+1)} \end{bmatrix} \tag{31}$$

$$\underline{\tilde{C}}_1^n = \begin{bmatrix} 0_{1\times H} & 1 & 0_{1\times S} \\ C & 0_{S\times 1} & I_{S\times S} \end{bmatrix} \tag{32}$$

We aim at designing an LQR/LQI for the new augmented system. In this case, the system is characterised by $m+1$ marginally stable modes ($\lambda = 1$) and the stabilisability and detectability conditions as explained in the Hautus-test [14] are again satisfied similarly to the previous case.

The resulting optimal gain is

$$\tilde{K}_1^n = \begin{bmatrix} K_1 & K_{C1} & K_{I1} \end{bmatrix} \tag{33}$$

We implement our control logic by switching gains $\tilde{K}$ and $\tilde{K}_1^n$ according to a threshold on the maximum on-ramp flow. Namely, we employ $\tilde{K}_1^n$ while $u_m^{max} < u_m^{\text{thres}}$ and $\tilde{K}$ otherwise.

IV. Setup for Experiment

A. Model of nonlinear multi-lane traffic flow

We provide simulation tests utilizing a model of first-order flow of traffic based on [14] to test and assess the performance of the suggested control technique. The model is used to simulate traffic behavior on a multi-lane highway and includes: (i) non-linear capacities for lateral flows of physically determined vehicles (which may likewise go about as disturbances for the established regulator); (ii) a Cell Transmission Models (CTM) system used for longitudinal flow; and (iii) a non-linear detailing to represent the capacity drop peculiarity. We momentarily survey the preservation regulation condition (1),

that all variable are explained of in Section II. Lateral flow with respect to manual lane-changing, indicated as $\bar{f}_{i,j}^{M}(k)$ are assumed among contiguous lanes of a similar section, and matching guidelines are characterized to allot and bound their qualities really. They are determined as

$$\bar{f}_{i,j}^{\mathrm{M}}(k) = l_{i,j,j+1}(k) - l_{i,j+1,j}(k), \tag{34}$$

where

$$l_{i,\bar{j},j}(k) = \min\left\{1, \frac{E_{i,j}(k)}{D_{i,j-1,j}(k) + D_{i,j+1,j}(k)}\right\} D_{i,\bar{j},j}(k) \tag{35}$$

$$E_{i,j}(k) = \frac{L_i}{T}\left[\rho_{i,j}^{\text{jam}} - \rho_{i,j}(k)\right] \tag{36}$$

$$D_{i,j}(k) = \frac{L_i}{T}\rho_{i,j}(k) A_{i,j,\bar{j}}(k) \tag{37}$$

$$A_{i,j,\bar{j}}(k) = \mu \ \max\left\{0, \frac{G_{i,j,\bar{j}}(k)\rho_{i,j}(k) - \rho_{i,\bar{j}}(k)}{G_{i,j,\bar{j}}(k)\rho_{i,j}(k) + \rho_{i,\bar{j}}(k)}\right\}, \tag{38}$$

and $\bar{j} = j \pm 1$. E defines the available space, in terms of flow acceptance, while D defines the lateral demand flow, calculated through the attractiveness rate's definition A. The equation (35) allows for the possibility of a limited space that is insufficient to allow lateral flow to enter from both sides of a cell. Regarding (38), the component G is generally equivalent to 1, suggesting that drivers mean to move to a quicker lane (prompting equivalent densities in lanes), However, it can also be tweaked to indicate specific area subordinate consequences, such as lateral flow toward a corridor from a lower to a greater density (for example upstream of on as well as off-ramps); while μ is a steady proportion in the scope of $[0, 1]$ implying lane-changing "aggression".

Longitudinal flows are streams that move starting with one cell then onto the next downstream cell while remaining in a similar lane. To deliver a more reasonable way of behaving at low densities, the Godunov-discretised first-order model recommended in [14] is utilized, For under-critical densities, however, a non-linear logarithmic demand model is used. A linearly falling demand formula for well over volumes and a linear decrease of the most extreme stream as a component of injected lateral inflows are also included in this model [25]. The general definition for longitudinal flow is

$$q_{i,j}(k) = \min\left\{Q_{i,j}^{D}(k), Q_{i+1,j}^{E}(k) - d_{i,j}(k)\right\}, \tag{39}$$

where

$$Q_{i,j}^{D}(k) = \begin{cases} v_{i,j}^{\max} \exp\left[-\frac{1}{\alpha}\left(\frac{\rho_{i,j}(k)}{\rho_{i,j}^{\text{cr}}}\right)^{\alpha}\right]\rho_{i,j}(k), & \text{if } \rho_{i,j}(k) < \rho_{i,j}^{\text{cr}} \\ \frac{(1-\gamma)Q_{i,j}^{\text{cap}}}{\rho_{i,j}^{\text{cr}} - \rho_{i,j}^{\text{jam}}}\left[\rho_{i,j}(k) - \rho_{i,j}^{\text{jam}}\right] + Q_{i,j}^{B}(k), & \text{otherwise} \end{cases} \tag{40}$$

$$Q_{i+1,j}^{E}(k) = \begin{cases} Q_{i+1,j}^{\text{cap}}, & \text{if } \rho_{i+1,j}(k) < \rho_{i+1,j}^{\text{cr}} \\ w_{i+1}\left[\rho_{i+1,j}^{\text{jam}} - \rho_{i+1,j}(k)\right], & \text{otherwise.} \end{cases} \tag{41}$$

$$Q_{i,j}^{B}(k) = \gamma\, Q_{i,j}^{\text{cap}} - \eta\left[l_{i,j+1,j}(k) + l_{i,j-1,j}(k)\right] \tag{42}$$

Parameter $v^{\max}$ shows the maximum speed, Q^{cap} defines the capacity flow, ρ^{cr} denotes the critical density (i.e., the density in which the capacity flow happens), while $\alpha = \left(\ln \frac{Q^{\text{cap}}}{v^{\max}\rho^{\text{cr}}}\right)^{-1}$ [14]. The parameter γ impacts the impact of capacity drop due to overcritical densities, whereas the parameter η affects capacity decline due to entering lateral flows. it is noted, by configuring $\gamma = 1$ and $\eta = 0$, we reach a conventional first-order model, i.e. no capacity drop happens at the head of congestion.

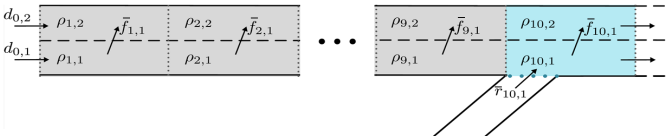

Fig. 2: The motorway segmentation used in the simulation experiments.

B. Network definition and simulation parameters

To test and assess the efficacy of the suggested technique, we consider a hypothetical two-lane highway section, as depicted in Fig. 2. Particularly, we examine a network contains ten segments with the same length $L_i = 0.5$ km, while a period step $T = 10$s is used. Various lanes highlight various boundaries, specifically an alternate FD, which might imply another traffic composition (e.g., countless heavy vehicles decreasing the capacity of a particular lane). Besides, the pre-owned traffic demand is portrayed in Fig. 3.

We present parameter $\Phi^{crt}(k)$ to define whether or not the controller is used at time k ($\Phi^{crt}(k) = 1$) or not ($\Phi^{crt}(k) = 0$), reflecting the scenario of using the designed lateral flows in our simulation runs. Furthermore, when we use our controller, 50 % of the vehicles are supposed to be connected and automated, so a portion of the controlled lane-changing flow is assumed as extra noise. Variety percentages of controlled vehicles are being examined, and it is expected that more percentage of autonomous vehicles leads in a less TTS. As a result, the used lateral flow for the simulations run is configures as

$$\bar{f}_{i,j}(k) = \begin{cases} \bar{f}_{i,j}^{\mathrm{M}}(k), & \text{if } \Phi^{crt}(k) = 0, \\ \text{sat}\left(f_{i,j}(k)\right) + 0.5\bar{f}_{i,j}^{\mathrm{M}}(k), & \text{if } \Phi^{crt}(k) = 1. \end{cases} \tag{43}$$

Because ramp-metering activities may cause a backlog to form outside of the highway network, we propose the following dynamics for the queue length $w(k)$ (in veh).

$$w(k+1) = w(k) + T\left(g_{10,1}(k) - r_{10,1}(k)\right), \tag{44}$$

where $g_{10,1}(k)$ is the demand for on-ramps during time intervals $(k, k+1]$. In our simulations, we use the following ramp flow

$$\bar{r}_{10,1}(k) = \begin{cases} g_{10,1}(k), & \text{if } \Phi^{crt}(k) = 0, \\ sat\left(r_{10,1}\right)(k), & \text{if } \Phi^{crt}(k) = 1. \end{cases} \tag{45}$$

It should be noticed that the influenced the outcome are bound by the following constraints.:

$$\text{sat}(f_{i,j}) = \begin{cases} f_{i,j}^{\min} = -\frac{L_i}{T}\rho_{i,j} & \text{if } f_{i,j} \le f_{i,j}^{\min} \\ f_{i,j}^{\max} = \frac{L_i}{T}\rho_{i,j} & \text{if } f_{i,j} \ge f_{i,j}^{\max} \\ f_{i,j}, & \text{otherwise;} \end{cases} \tag{46}$$

TABLE I: The employed parameters in the nonlinear multi-lane traffic flow model.

	$v^{\max}$ [km/h]	Q^{cap} [veh/h]	ρ^{cr} [veh/km]	ρ^{jam} [veh/km]	γ	η	G	μ
$j=1$	100	1800	22	120	0.6	0.8	1	0.6
$j=2$	100	2400	26	160	0.6	0.8	1	0.6

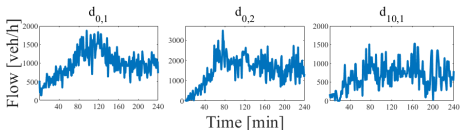

Fig. 3: The employed traffic demand in the simulation experiments.

$$\text{sat}(r_{10,1}) = \begin{cases} r_{10,1}^{\min} = 0, & \text{if } r_{10,1} \le r_{10,1}^{\min} \\ r_{10,1}^{\max} = \min\left(\frac{w}{T} + D_{10,1}, Q_1^{\text{cap}}\right), & \text{if } r_{10,1} \ge r_{10,1}^{\max} \\ r_{10,1}, & \text{otherwise.} \end{cases} \tag{47}$$

V. Experiment Results

A. No-control case

The nonlinear traffic model's implementation (34)-(42) in this specified network defines the no-control case. Figs. 4(top) and 5(top) shows a significant congestion starts at the bottleneck area located at segment 10 and moves back to the segment 1. The congestion happens because of two reasons as a) the significant volume of traffic approaching from the ramp, because the whole demand is approximately 4600 veh/h during the peak period, while entire capacity is 4200 veh/h; same as b) the inefficient "natural" flow of lane-changing. Capacity drops also occur at the locations of bottleneck units in the highway network, causing congestion to worsen.

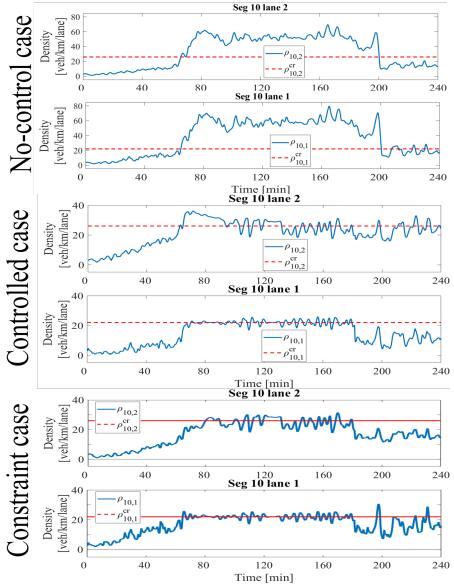

Fig. 4: Bottlenecks' density. (top) The no-control case. (middle) The controlled case. (bottom) The constraint case.

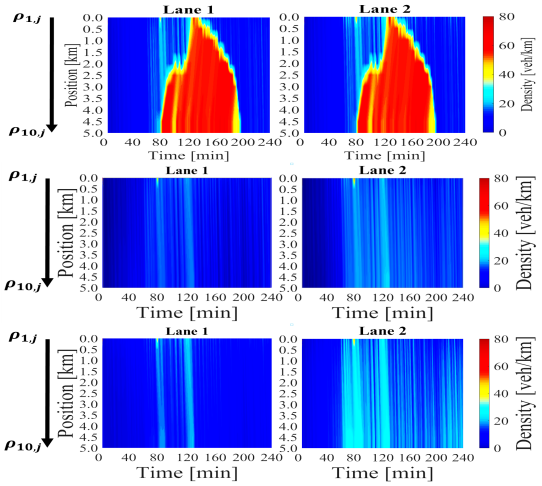

Fig. 5: Contour plots of densities. (top) The no-control case. (middle) The controlled case. (bottom) The constraint case.

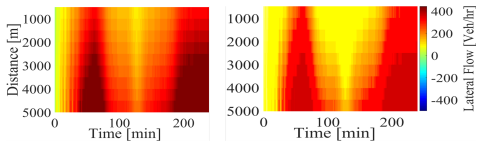

Fig. 6: Contour plots of lateral flows in the controlled case; without considering the ramp saturation (left) and with considering the ramp saturation (right).

B. Controller for lateral flow and ramp metering

We use Tajdari's method [14], employs the linear dynamic compensator (21), (22) to the model of nonlinear traffic (34)-(42). A set of experiments have been performed to assess the controller's sensitivity to the parameters selection as w_Q, w_{R_1} and w_{R_2}. As a result, for a wide range of parameter values, the controller exhibits satisfactory performance in terms of Total Time Spent (TTS), as measured by [14]. Here are the findings obtained with $w_Q = 1$, $w_{R_1} = 1$ and $w_{R_2} = 0.001$. Congestion completely avoided and the the bottleneck area's densities maintained at their critical values, according to Figs. 4(middle) and 5(middle). The outputs of control are determined and proposed throughout the duration of the simulation experiment to ensure that critical density is not exceeded. In addition, during the peak period, a big line is formed at the on-ramp, which in our research is not upper-bounded (see Fig. 7). The improvement of TTS is approximately 26% (see Table II).

C. Ramp-metering flow saturation control

To compare the effect of considering the ramp-metering saturation, we integrate the control gain in (33) to the controller in the previous section. As explained in Section III-C,

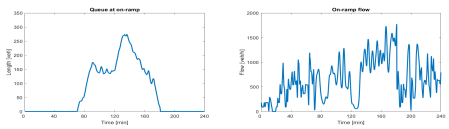

Fig. 7: The queue of ramp (left) and flow of ramp (right) in the controlled case.

TABLE II: TTS report.

Case	No control	Considering no saturation (Tajdari's method [14])	Considering saturation (our method)
TTS $[veh.hr]$	1060	783	665
Improvement $(\%)$		26	37

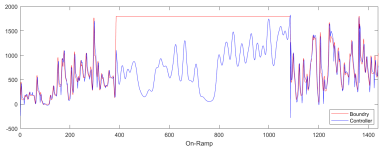

Fig. 8: Controlled on-ramp input in the constrained case.

the controller switches from the gain in (20) to gain in (33) when the ramp-metering flow is close to saturation. The rest of the control parameters w_Q, w_{R_1} and w_{R_2} are same as the controller in Section V-B. Here, the congestion is likewise completely gone, and the densities in the bottleneck location remain at critical levels, see Figs. 4(bottom) and 5(bottom). Density control plots are shown in the figures to ensure that critical set-point value is tracked and maintained throughout the simulation phase. The TTS improvement is about 37% (see also Table II). Furthermore, we showed in Fig. 8 that how the on-ramp flow is controlled considering the saturation.

VI. Conclusions

The paper proposes an integrated approach for changing lanes and metering ramps on highways experiencing bottlenecks. In the used model for assessing the controller the existence of connected vehicles and partially autonomous vehicles are considered. Simulation tests using the first order, the multi lanes, and the flow of macroscopic traffic models that include capacity drop phenomena are used to demonstrate the effectiveness of the proposed approach. A future publication will investigate the controller's stability features, and robustness of the controller for variety of parameter choices.

References

[1] F. Tajdari, C. Roncoli, N. Bekiaris-Liberis, and M. Papageorgiou, "Integrated ramp metering and lane-changing feedback control at motorway bottlenecks," in *2019 18th European Control Conference (ECC)*. IEEE, 2019, pp. 3179–3184.

[2] C. Diakaki, M. Papageorgiou, I. Papamichail, and I. K. Nikolos, "Overview and analysis of vehicle automation and communication systems from a motorway traffic management perspective," *Transportation Research Part A*, vol. 75, pp. 147 – 165, 2015.

[3] F. Tajdari, A. Golgouneh, A. Ghaffari, A. Khodayari, A. Kamali, and N. Hosseinkhani, "Simultaneous intelligent anticipation and control of follower vehicle observing exiting lane changer," *IEEE Transactions on Vehicular Technology*, vol. 70, no. 9, pp. 8567–8577, 2021.

[4] F. Tajdari, A. Ghaffari, A. Khodayari, A. Kamali, N. Zhilakzadeh, and N. Ebrahimi, "Fuzzy control of anticipation and evaluation behaviour in real traffic flow," in *2019 7th International Conference on Robotics and Mechatronics (ICRoM)*. IEEE, 2019, pp. 248–253.

[5] F. Tajdari, N. E. Toulkani, and M. Nourimand, "Intelligent architecture for car-following behaviour observing lane-changer: Modeling and control," in *2020 10th International Conference on Computer and Knowledge Engineering (ICCKE)*. IEEE, 2020, pp. 579–584.

[6] A. Ghaffari, A. Khodayari, A. Kamali, F. Tajdari, and N. Hosseinkhani, "New fuzzy solution for determining anticipation and evaluation behavior during car-following maneuvers," *Proceedings of the Institution of Mechanical Engineers, Part D: Journal of automobile engineering*, vol. 232, no. 7, pp. 936–945, 2018.

[7] A. Khodayari, A. Ghaffari, A. Kamali, and F. Tajdari, "A new model of car following behavior based on lane change effects using anticipation and evaluation idea," *Iranian Journal of Mechanical Engineering Transactions of the ISME*, vol. 16, no. 2, pp. 26–38, 2015.

[8] E. Amini, A. Omidvar, and L. Elefteriadou, "Optimizing operations at freeway weaves with connected and automated vehicles," *Transportation Research Part C: Emerging Technologies*, vol. 126, p. 103072, 2021.

[9] F. Tajdari and C. Roncoli, "Adaptive traffic control at motorway bottlenecks with time-varying fundamental diagram," *IFAC-PapersOnLine*, vol. 54, no. 2, pp. 271–277, 2021.

[10] F. Tajdari, M. Kabganian, E. Khodabakhshi, and A. Golgouneh, "Design, implementation and control of a two-link fully-actuated robot capable of online identification of unknown dynamical parameters using adaptive sliding mode controller," in *2017 Artificial Intelligence and Robotics (IRANOPEN)*. IEEE, 2017, pp. 91–96.

[11] F. Tajdari, N. E. Toulkani, and N. Zhilakzadeh, "Semi-real evaluation, and adaptive control of a 6dof surgical robot," in *2020 11th Power Electronics, Drive Systems, and Technologies Conference (PEDSTC)*. IEEE, 2020, pp. 1–6.

[12] T. Bahram, G. Alireza, T. Farzam, and K. Erfan, "A novel online method for identifying motion artifact and photoplethysmography signal reconstruction using artificial neural networks and adaptive neuro-fuzzy inference system," *Neural Computing & Applications*, vol. 32, no. 8, pp. 3549–3566, 2020.

[13] C. Roncoli, M. Papageorgiou, and N. Bekiaris-Liberis, "Lane-changing feedback control for efficient lane assignment at motorway bottlenecks," *Transportation Research Record*, vol. 2625, pp. 20–31, 2017.

[14] F. Tajdari, C. Roncoli, and M. Papageorgiou, "Feedback-based ramp metering and lane-changing control with connected and automated vehicles," *IEEE Transactions on Intelligent Transportation Systems*, 2020.

[15] F. Tajdari, M. Tajdari, and A. Rezaei, "Discrete time delay feedback control of stewart platform with intelligent optimizer weight tuner," in *2021 IEEE International Conference on Robotics and Automation (ICRA)*. IEEE, 2021, pp. 12 701–12 707.

[16] F. Tajdari and N. Ebrahimi Toulkani, "Implementation and intelligent gain tuning feedback–based optimal torque control of a rotary parallel robot," *Journal of Vibration and Control*, p. 10775463211019177, 2021.

[17] F. Tajdari, M. Kabganian, N. F. Rad, and E. Khodabakhshi, "Robust control of a 3-dof parallel cable robot using an adaptive neuro-fuzzy inference system," in *2017 Artificial Intelligence and Robotics (IRANOPEN)*. IEEE, 2017, pp. 97–101.

[18] Y. Yang, T. Yuan, T. Huysmans, W. S. Elkhuizen, F. Tajdari, and Y. Song, "Posture-invariant three dimensional human hand statistical shape model," *Journal of Computing and Information Science in Engineering*, vol. 21, no. 3, 2021.

[19] F. Tajdari, T. Huysmans, Y. Yang, and Y. Song, "Feature preserving non-rigid iterative weighted closest point and semi-curvature registration," *IEEE Transactions on Image Processing*, vol. 31, pp. 1841–1856, 2022.

[20] M. Tajdari, A. Pawar, H. Li, F. Tajdari, A. Maqsood, E. Cleary, S. Saha, Y. J. Zhang, J. F. Sarwark, and W. K. Liu, "Image-based modelling for adolescent idiopathic scoliosis: mechanistic machine learning analysis and prediction," *Computer methods in applied mechanics and engineering*, vol. 374, p. 113590, 2021.

[21] R. L. Williams and D. A. Lawrence, *Linear state-space control systems*. Hoboken, NJ, USA: John Wiley & Sons, Inc., 2007.

[22] F. Tajdari, N. E. Toulkani, and N. Zhilakzadeh, "Intelligent optimal feedback torque control of a 6dof surgical rotary robot," in *2020 11th Power Electronics, Drive Systems, and Technologies Conference (PEDSTC)*. IEEE, 2020, pp. 1–6.

[23] J. G. da Silva Jr and S. Tarbouriech, "Anti-windup design with guaranteed regions of stability for discrete-time linear systems," *Systems & Control Letters*, vol. 55, no. 3, pp. 184–192, 2006.

[24] F. Tajdari, E. Khodabakhshi, M. Kabganian, and A. Golgouneh, "Switching controller design to swing-up a two-link underactuated robot," in *2017 IEEE 4th International Conference on Knowledge-Based Engineering and Innovation (KBEI)*. IEEE, 2017, pp. 0595–0599.

[25] T. Yuan, F. Alasiri, and P. A. Ioannou, "Selection of the speed command distance for improved performance of a rule-based vsl and lane change control," *IEEE Transactions on Intelligent Transportation Systems*, 2022.